

# Epoxy Networks Containing Large Mass Fractions of a Monofunctional Polyhedral Oligomeric Silsesquioxane (POSS)

María J. Abad,<sup>†</sup> Luis Barral,<sup>†</sup> Diana P. Fasce,<sup>‡</sup> and Roberto J. J. Williams<sup>\*,‡</sup>

*Institute of Materials Science and Technology (INTEMA), University of Mar del Plata and National Research Council (CONICET), J. B. Justo 4302, 7600 Mar del Plata, Argentina, and Departamento de Física, Escuela Universitaria Politécnica de Ferrol, Universidad de A Coruña, Av. 19 de Febrero s/n, 15405 Ferrol, Spain*

*Received September 30, 2002; Revised Manuscript Received March 5, 2003*

**ABSTRACT:** A polyhedral oligomeric silsesquioxane (POSS) containing one epoxy group and seven isobutyl groups per molecule was incorporated into an epoxy network following a two-stage process. In the first stage, POSS was reacted with an aromatic diamine, employing a 1:1 molar ratio of both reactants. The distribution of species at the end of reaction, determined by size exclusion chromatography (SEC), was close to the ideal one. In a second step, this precursor was reacted with the stoichiometric amount of an aromatic diepoxide to generate an organic–inorganic hybrid material containing 51.8 wt % POSS. A primary liquid–liquid phase separation process occurred at the time of adding the diepoxide to the POSS–diamine precursor. This led to a macrophase separation into epoxy-rich and POSS-rich regions, possibly derived from the incompatibility of the isobutyl groups attached to the POSS with the aromatic epoxy–amine network. A secondary phase separation occurred in the epoxy-rich phase in the course of polymerization, producing a dispersion of small POSS domains. Both modulated local thermal analysis (LTA) and differential scanning calorimetry (DSC) showed that most POSS-rich domains were amorphous. A small fraction of POSS crystals was also detected. A postcure cycle led to an increase in the glass transition temperature and the disappearance of crystallinity. A reference network was synthesized by replacing POSS by phenyl glycidyl ether (PGE) in equimolar amounts. The resulting network was homogeneous but exhibited a lower glass transition temperature than the POSS-modified network. As both networks had the same topology, the higher  $T_g$  observed for the POSS-modified epoxy may be associated with the hindering of polymer chain motions by their covalent bonding to POSS clusters. The most important concept arising from these results is that a phase separation process may take place when employing a POSS bearing organic groups that are not compatible with the epoxy network.

## Introduction

Polyhedral oligomeric silsesquioxanes (POSS),  $(\text{RSiO}_{1.5})_n$  with  $n = 6, 8, 10, \dots$ , are nanosized cage structures that can be incorporated into linear or thermosetting polymers to improve their thermal and oxidation resistance, and reduced flammability.<sup>1–9</sup> Octahedra ( $n = 8$ ) are the most representative members of this family. Depending on the number of organic groups (R) bearing reactive functionalities, POSS can be classified as nonfunctional, monofunctional or polyfunctional. Monofunctional POSS are usually synthesized by a corner capping reaction of a trisilanol,  $\text{R}_7\text{Si}_7\text{O}_9(\text{OH})_3$ , containing seven nonreactive organic groups such as  $\text{C-C}_5\text{H}_9$ ,  $\text{C-C}_6\text{H}_{11}$ , and  $\text{i-C}_4\text{H}_9$ , with  $\text{R}'\text{SiX}_3$ , where R' bears a reactive site (vinyl, allyl, isocyanate, epoxy, etc.) and X = halogen or alkoxide.<sup>3,6</sup> The introduction of such nanoscaled POSS macromers into an organic polymer by polymerization at the single reactive site (one of the eight corner groups in a POSS macromer), leads to POSS-modified polymers.

The use of monofunctional POSS to improve properties of linear polymers, such as methacrylates, styrenics, norbornenes, ethylenes, propylenes, and urethanes, has been extensively reported.<sup>4,10–20</sup> Star polymers have been synthesized via atom transfer radical polymerization of methyl methacrylate using octafunctional POSS cores.<sup>21</sup> Polyfunctional POSS were polymerized to obtain

polymer networks with the POSS cage acting as the basic cross-linking unit.<sup>22–25</sup> However, few reports have been published regarding the incorporation of monofunctional POSS into thermosetting polymers. Epoxy networks were modified with 5 or 10 wt % monofunctional POSS containing one epoxy group per cage.<sup>26,27</sup> After chemical reaction with the hardener (a diamine), POSS cages remained as pendant groups in the polymer network. The introduction of these bulky structures led to a slight increase of the glass transition temperature and retarded the physical aging process in the glassy state.

The aim of this work was to examine the possibility of incorporating large mass fractions of POSS cages as pendant groups in an epoxy network and to analyze the structures and thermal properties of the resulting organic–inorganic hybrid materials.

## Experimental Section

**Materials.** The chemical structure of the selected POSS is shown in Figure 1. It is a glycidylisobutyl–POSS from Hybrid Plastics (EPO 418), bearing seven isobutyl groups and one epoxy group. Its chemical formula is  $\text{C}_{34}\text{H}_{74}\text{O}_{14}\text{Si}_8$ , with a molar mass of 931.63 g/mol. Its appearance is a white powder, and it is soluble in solvents such as tetrahydrofuran, chloroform, and hexane but insoluble in acetonitrile.  $^1\text{H}$  and  $^{13}\text{C}$  NMR spectra confirmed the reported chemical structure.

Phenyl glycidyl ether (PGE) from Sigma-Aldrich was used to synthesize a reference polymer network for comparison purposes, where the monofunctional POSS was replaced by an equivalent amount of PGE. The synthesis of a polymer network required the use of a diepoxide. The selected one was

\* Corresponding author. E-mail: williams@fi.mdp.edu.ar.

<sup>†</sup> Escuela Universitaria Politécnica de Ferrol.

<sup>‡</sup> INTEMA.

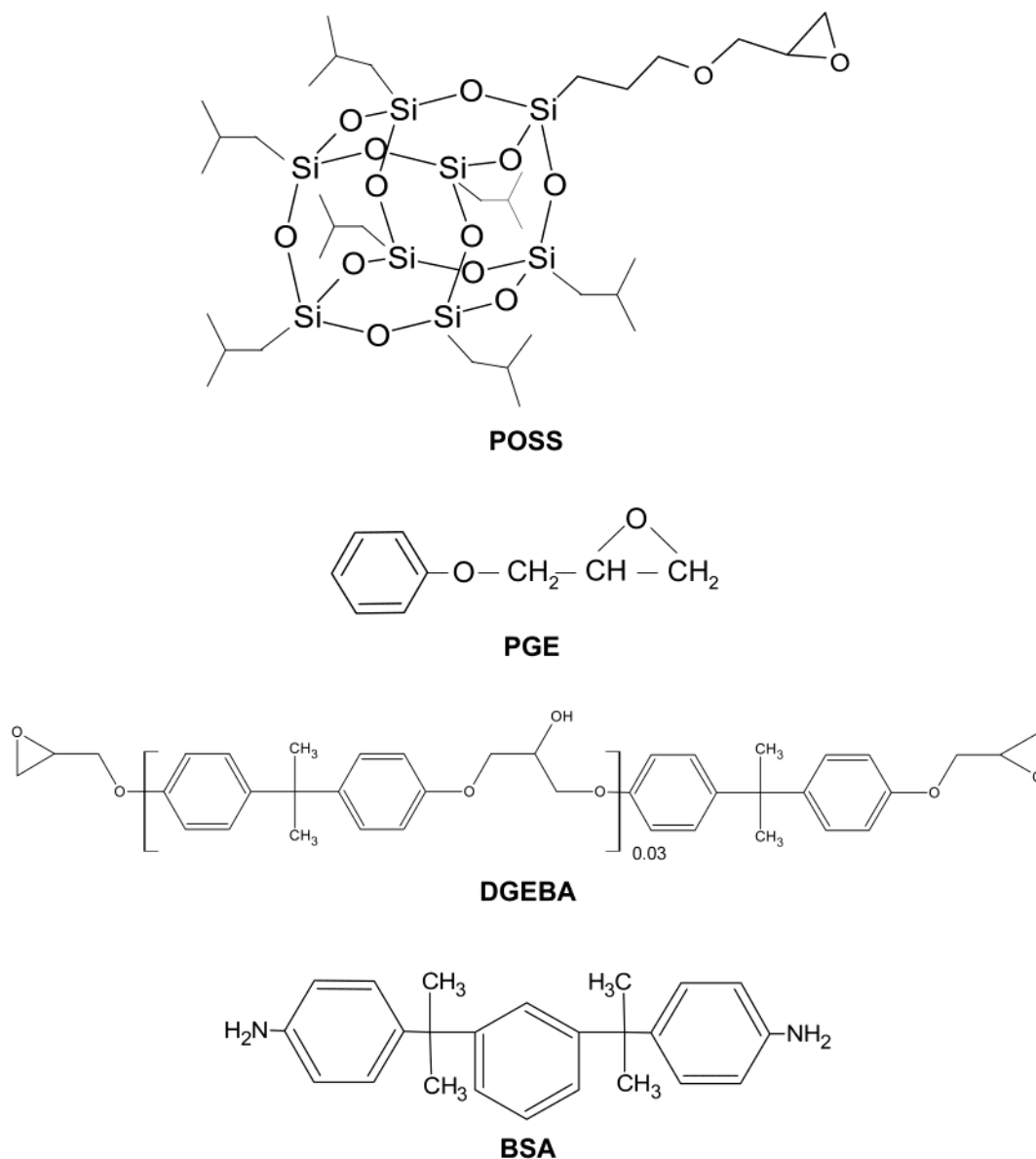


**Figure 1.** Chemical structures of POSS, PGE, DGEBA, and BSA.

based on diglycidyl ether of bisphenol A (DGEBA, MY790 Ciba), with a molar mass of 348 g/mol (Figure 1).

The diamine used as a hardener was 4,4'-[1,3 phenylenebis(1-methylethylidene)]bis(aniline) (BSA, Ken Seika Corp., 99% purity, molar mass = 344 g/mol). Its chemical structure is also shown in Figure 1. Its melting temperature was 116 °C as determined from differential scanning calorimetry (DSC).

**Synthesis of POSS-Modified DGEBA—BSA Epoxy Networks.** The synthesis was performed in two steps. In the first step, POSS (4.658 g) and BSA (1.720 g), were reacted in equimolar proportions (1 mol of POSS per mole of BSA). Both reactants were first dissolved in tetrahydrofuran (THF), and the solvent was evaporated at 65 °C. The resulting solid was milled, heated to 160 °C, and kept at this temperature for 2 h to complete the epoxy—amine reaction. The polymer network was synthesized by adding the stoichiometric amount of DGEBA (2.610 g, representing 1.5 mol of DGEBA per initial mole of BSA), mixing at about 115 °C, pouring the solution into an open aluminum mold, and curing for 30 min at 115 °C and 60 min at 125 °C. Some samples were postcured at 140 °C during 22 h. The POSS fraction in the resulting polymer network was 51.8 wt %.

**Synthesis of PGE-Modified DGEBA—BSA Networks.** The synthesis was performed in two steps. In the first step, PGE (1.50 g) and BSA (3.44 g) were mixed at 90 °C in a 1:1

molar ratio, and reacted at 120 °C during 45 min to complete conversion. The polymer network was synthesized by adding the stoichiometric amount of DGEBA (5.22 g, representing 1.5 mol of DGEBA per initial mole of BSA), mixing at 90 °C, pouring the solution into an open aluminum mold, and curing for 30 min at 115 °C and 60 min at 125 °C. The PGE mass fraction in the resulting polymer network was 14.8 wt %.

**Techniques.** Reactions were followed by size exclusion chromatography (SEC). A set of glass tubes containing known masses of the reacting mixture, in the range of 15 mg, were placed in a thermostat at the desired temperature. Tubes were removed at predetermined times, their contents were dissolved in 5 mL of tetrahydrofuran (THF), and 100  $\mu$ L of the resulting solution was injected into the size exclusion chromatograph (SEC, Waters 510 with HR 0.5, 1, and 3 Ultrastayragel columns, UV detector at 254 nm, and a THF flow rate of 1 mL/min).

<sup>29</sup>Si NMR spectra of the starting POSS and of its reaction product with BSA were performed in CDCl<sub>3</sub> and recorded on a Bruker AM 500 NMR spectrometer operated at 99.36 MHz. TMS was used as external reference.

Thermal characterization of reactants, intermediate products, and final materials was performed using differential scanning calorimetry (DSC, Perkin-Elmer Pyris 1, calibrated with indium, using heating and cooling scans at 10 °C/min under a nitrogen atmosphere) and thermal gravimetric analy-

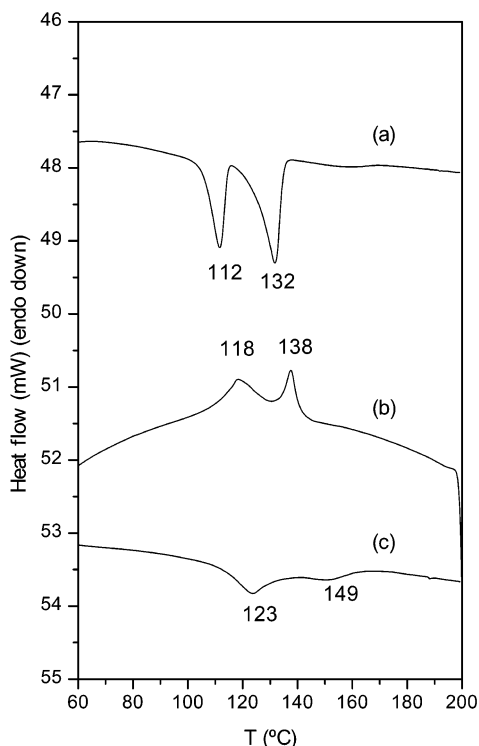


**Figure 2.** DSC thermograms of POSS: (a) first heating scan; (b) cooling scan; (c) second heating scan.

sis (TGA7, Perkin-Elmer, calibrated with nickel and perkallo, performing dynamic runs at 10 °C/min or isothermal runs under argon). The microscopic thermal behavior of the samples was examined with a microthermal analyzer ( $\mu$ TA 2990, TA Instruments), working in the scanning thermal microscopy (SThM) mode. This mode allowed us to obtain thermal conductivity images and perform modulated local thermal analysis (LTA) of the samples. In the LTA mode, the thermal probe was placed at the selected domains and thermal properties were measured by modulating the probe temperature with a frequency of 5 Hz and an amplitude of 10 °C. The probe-temperature calibration was performed using room temperature (23 °C) and the melting point of a standard certified sample of poly(ethylene terephthalate) as calibration points.<sup>28</sup>

Dynamic mechanical spectra of the POSS-modified epoxy network were obtained with a Perkin-Elmer DMA-7 system, operating at 1 Hz in both the three-point-bending and compression modes, using a 10 °C/min heating rate.

Morphologies of the POSS-modified epoxy network were observed both by atomic force microscopy (AFM mode of the  $\mu$ TA 2990, TA Instruments) and by scanning electron microscopy (SEM, JEOL JSM 35CF, gold-coated fracture surfaces). AFM micrographs were obtained by scanning an area of 100  $\times$  100  $\mu\text{m}^2$  with a scan rate of 100  $\mu\text{m}/\text{s}$  and an image resolution of 400 pixels.

## Results and Discussion

**Thermal Characterization of POSS.** Two well-defined melting peaks, at 112 and 132 °C, are shown in the DSC thermogram of the commercial product (Figure 2a). Crystallization peaks at 138 °C and 118 °C, were present in a subsequent cooling scan (Figure 2b), leading to melting peaks at 123 and 149 °C, in the second heating scan (Figure 2c). Subsequent cooling and heating cycles did not modify the thermograms shown in Figure 2, parts b and c. The heat of melting, calculated from the areas under both peaks in heating scans, was 20.6 J/g for the first scan and 15.9 J/g for the second scan.

The presence of two well-defined melting peaks is possibly due to the formation of two different crystalline phases. Figure 3 shows an AFM micrograph of crystals present in the commercial product. LTA of POSS crystals showed the presence of two melting processes (Figure 4). Depending on the probe location, one or both melting processes were observed. The higher melting temperature was always measured at the center of the crystals while in the boundaries of individual crystals, the two melting temperatures or only the lower one were obtained.

The thermal stability of POSS was analyzed using TGA (Figure 5). A significant thermal degradation was evidenced from 220 °C, although weight loss was also observed in the course of isothermal runs at 200 °C. POSS could withstand repeated heating/cooling cycles at 10 °C/min, up to 200 °C, without exhibiting any significant change in DSC thermograms.

The temperature region comprising melting and degradation of the selected POSS defines its processability window. In our case, it was between about 140 and 180 °C. The strategy to introduce POSS into the epoxy network was to react it to completion, in a first step, with an excess of a diamine. The following diamines were screened in order to find a particular one whose complete reaction with POSS would take a few hours at 160 °C: 4,4'-diaminodiphenylmethane (DDM), 4,4'-methylenebis[3-chloro-2,6-diethylaniline] (MCDEA), and BSA. The reaction with DDM was relatively fast, the one with MCDEA was slow, and BSA reacted at an appropriate rate. The latter was the diamine finally selected.

**Molar Ratio of POSS/BSA.** The next step was to define a convenient stoichiometric ratio for the reaction mixture. On one hand, we wanted to introduce a large mass fraction of POSS into the epoxy network. However, the maximum amount should be limited by the following: (a) the need to obtain a product with a functionality-average functionality higher than 2, to generate a polymer network in the subsequent reaction with a diepoxide (second step), and (b) the need to minimize the fraction of BSA-(POSS)<sub>4</sub> (the four amine hydrogens of BSA reacted with POSS), because this species cannot be covalently bonded to the polymer network.

A convenient molar ratio of POSS/BSA was 1:1, representing a stoichiometric ratio of functionalities equal to 0.25. This ratio leads to a 51.8 wt % POSS in the final polymer network (obtained after reaction with the diepoxide). The distribution of reaction products may be estimated by assuming that the four amine hydrogens have equal reactivity and there are no substitution effects (for an aromatic diamine substitution effects are however expected).<sup>29</sup> For this case, the probability of finding a reacted position is 0.25 while the probability of finding an unreacted position is (1-0.25). This leads to the following ideal distribution of reaction products:

$$\text{BSA}/(\text{BSA})_0 = (1 - 0.25)^4 = 0.316$$

$$\text{BSA}-(\text{POSS})/(\text{BSA})_0 = 4(1 - 0.25)^3(0.25) = 0.422$$

$$\text{BSA}-(\text{POSS})_2/(\text{BSA})_0 = 6(1 - 0.25)^2(0.25)^2 = 0.211$$

$$\text{BSA}-(\text{POSS})_3/(\text{BSA})_0 = 4(1 - 0.25)(0.25)^3 = 0.047$$

$$\text{BSA}-(\text{POSS})_4/(\text{BSA})_0 = (0.25)^4 = 0.004$$

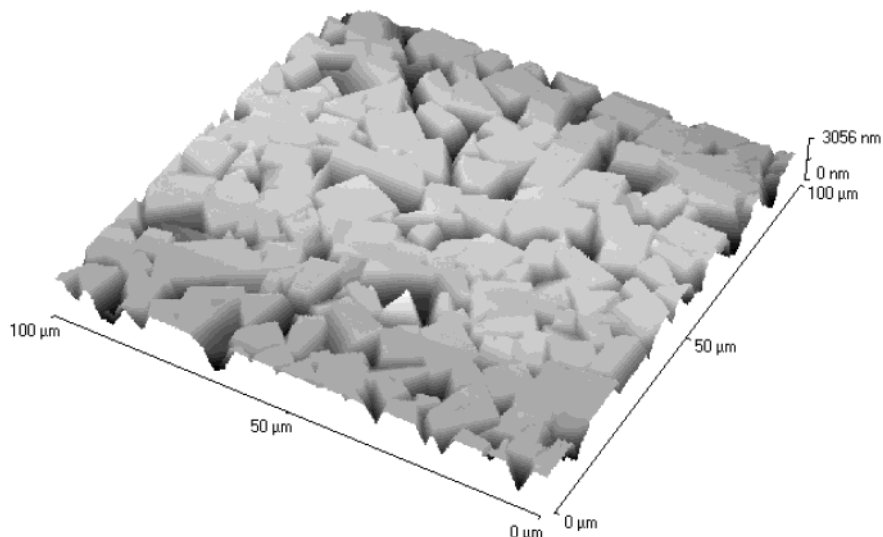


Figure 3. AFM micrograph of POSS crystals.

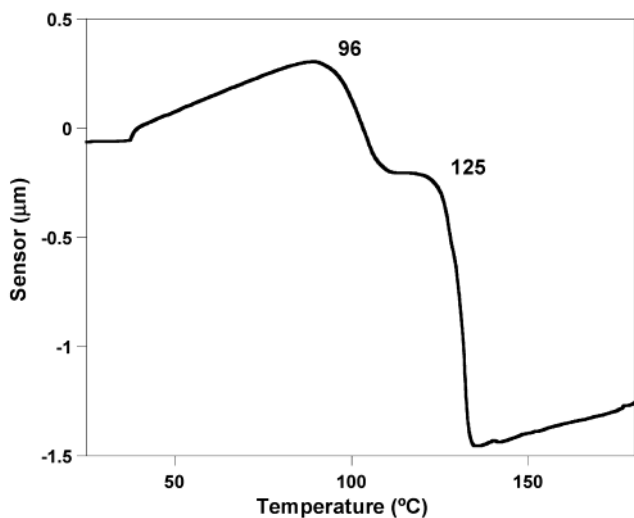


Figure 4. Local thermal analysis of POSS, showing the presence of two melting processes (sensor signal vs temperature at a scan rate: 10 °C/s).

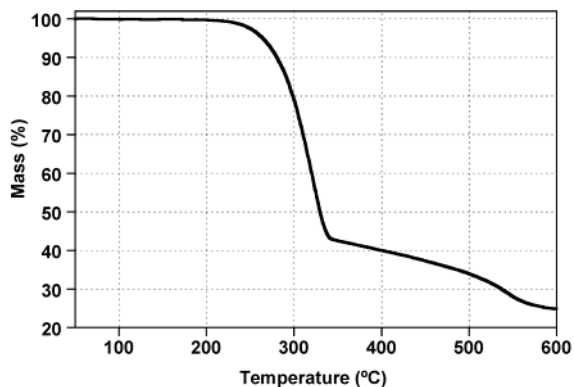


Figure 5. TGA thermogram of POSS at 10 °C/min, under Ar.

Therefore, in the final epoxy network, only 0.4% of the initial BSA will remain in the sol fraction.

The functionality-average functionality of the reaction product is given by<sup>29</sup>

$$\frac{\sum(4 - i)^2[\text{BSA}-(\text{POSS})_i]/(\text{BSA})_0}{\sum(4 - i)[\text{BSA}-(\text{POSS})_i]/(\text{BSA})_0} = 3.25$$

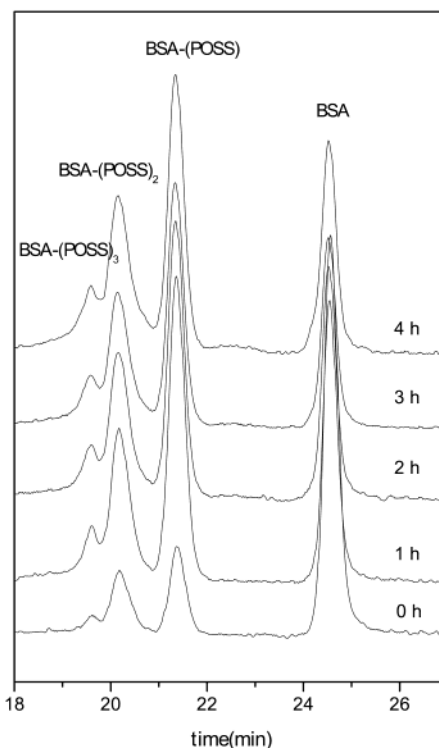


Figure 6. SEC chromatograms obtained at different times during the reaction of equimolar amounts of POSS and BSA, at 160 °C.

where the first term of both summations corresponds to  $i = 0$ .

**Analysis of the POSS–BSA Reaction Using SEC.** The reaction of equimolar amounts of POSS and BSA (stoichiometric ratio of POSS/BSA = 0.25), at 160 °C, was followed by SEC. Figure 6 shows the resulting chromatograms, at different reaction times. As POSS did not have any significant absorption at 254 nm, the signal of the UV detector was only sensitive to the amount of BSA. Therefore, the relative areas (or heights) of different peaks represent their molar fractions in the mixture.

At  $t = 0$  there was a significant conversion produced in the course of sample preparation. From  $t = 2$  h, the relative heights of peaks did not change within experi-



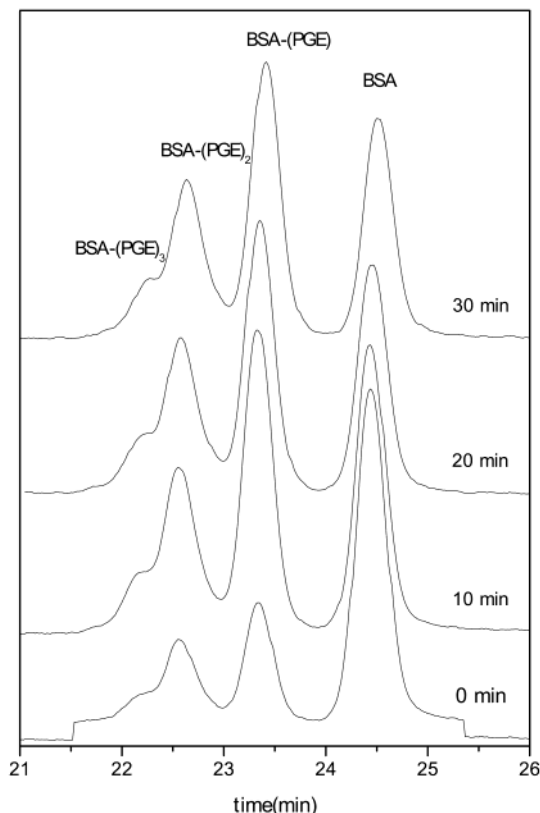


**Figure 7.** SEC chromatograms obtained at different times during the reaction of equimolar amounts of PGE and BSA, at 120 °C.

mental error. The corresponding molar fractions of reaction products were the following:

$$\text{BSA}/(\text{BSA})_0 = 0.32$$

$$\text{BSA}-(\text{POSS})/(\text{BSA})_0 = 0.41$$

$$\text{BSA}-(\text{POSS})_2/(\text{BSA})_0 = 0.23$$

$$\text{BSA}-(\text{POSS})_3/(\text{BSA})_0 = 0.04$$

$$\text{BSA}-(\text{POSS})_4/(\text{BSA})_0 = \text{undetected}$$

These values are in very good agreement with those expected for an ideal reaction.

**Analysis of the POSS–BSA Reaction Product Using  $^{29}\text{Si}$  NMR.** As amines might be capable of opening and oligomerizing POSS cages, it was considered appropriate to compare  $^{29}\text{Si}$  NMR spectra of the starting POSS and of its reaction product with BSA. In both spectra, three sharp peaks, with relative intensities 1:3:4, were present, respectively at  $-67.29$ ,  $-67.61$  and  $-67.83$  ppm (for POSS) and at  $-67.36$ ,  $-67.58$  and  $-67.81$  ppm (for POSS–BSA). This constitutes direct evidence of the integrity of POSS cages after reaction with BSA.

**Analysis of the PGE–BSA Reaction Using SEC.** To synthesize a reference network with POSS replaced by a monofunctional organic epoxide, equimolar amounts of PGE and BSA (stoichiometric ratio PGE/BSA = 0.25) were reacted at 120 °C. The evolution of SEC chromatograms is shown in Figure 7. The UV absorption of PGE at 254 nm is significantly lower than the one of BSA, so that the relative ratio of peak areas (heights) may be taken as the molar fractions of the different species.

At  $t = 0$ , there was a significant advance in the reaction, produced during the mixing stage. From  $t = 20$  min, no significant changes in the peak distribution were detected within experimental error. A reaction time,  $t = 45$  min, was arbitrarily selected to ensure that the reaction attains complete conversion.

The distribution of reaction products at complete conversion was the following:

$$\text{BSA}/(\text{BSA})_0 = 0.35$$

$$\text{BSA}-(\text{PGE})/(\text{BSA})_0 = 0.40$$

$$\text{BSA}-(\text{PGE})_2/(\text{BSA})_0 = 0.21$$

$$\text{BSA}-(\text{PGE})_3/(\text{BSA})_0 = 0.04$$

$$\text{BSA}-(\text{PGE})_4/(\text{BSA})_0 = \text{undetected}$$

A similar distribution as the one resulting from the BSA–POSS reaction, was obtained.

**Synthesis of POSS-Modified and PGE-Modified Epoxy Networks.** The synthesis of the POSS-modified epoxy network was performed by adding the stoichiometric amount of DGEBA (1.5 mol per mole of BSA), to the reaction product between POSS and BSA.

The POSS–BSA precursor was a one-phase system at the synthesis temperature (160 °C), but despite being covalently bonded to BSA, POSS crystallized when cooling below 90 °C (observed during DSC cooling scans at 10 °C/min). A temperature range comprised between 115 and 125 °C was selected for DGEBA addition, as a compromise to prevent POSS crystallization and to avoid a very fast polymerization rate. However, DGEBA addition produced an instantaneous phase separation, leading to an opaque liquid. Then, the epoxy–amine polymerization took place in a heterogeneous system.

The reaction at 125 °C was followed by SEC. Figure 8 shows the evolution of SEC chromatograms during the first 20 min reaction. At 25 min, the polymer had gelled. At  $t = 0$ , the reaction had already advanced as revealed by the appearance of the DGEBA–BSA reaction product. At  $t = 20$  min, soon before gelation, peaks of DGEBA, BSA, and DGEBA–BSA had decreased considerably and a tail of high molar mass products appeared in the SEC chromatogram.

The overall conversion attained in this reaction may be estimated from the amount of free DGEBA monomer remaining in solution.<sup>30</sup> Assuming that both epoxy groups have equal reactivities and there are no substitution effects, the fraction of unreacted DGEBA at a particular epoxy conversion,  $p$ , is given by the simultaneous probability that both epoxy groups remain unreacted:

$$d/c_0 = (1 - p)^2$$

where  $d/c_0$  is the actual area of the DGEBA peak with respect to the initial one, expressed per unit mass of sample. The conversion is then given by

$$p = 1 - (d/c_0)^{1/2}$$

As  $c_0$  could not be directly determined due to the advance in the reaction observed in the initial sample, a calibration curve was constructed using DGEBA solutions of known concentrations. Using the calibration curve, the ratio  $d/c_0$  could be determined for every

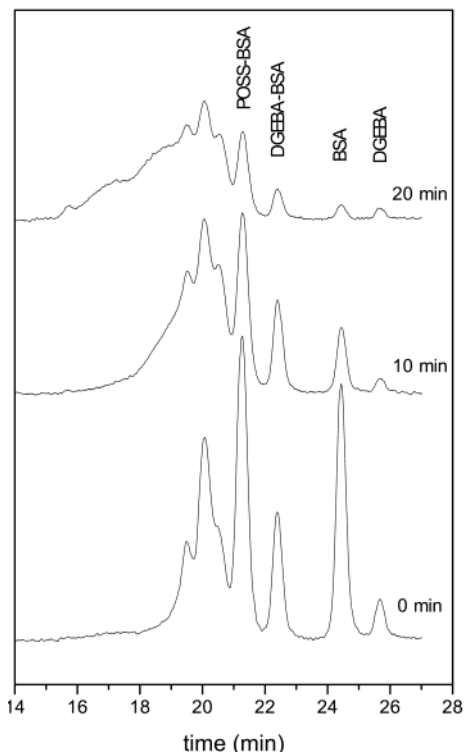


**Figure 8.** SEC chromatograms obtained at different times during the reaction of DGEBA with the reaction product between POSS and BSA, at 125 °C.

reaction time. For  $t = 20$  min, soon before gelation, the calculated conversion was  $p = 0.63$ . The theoretical gel conversion may be calculated from the functionalities of both reactants (for the POSS–BSA reaction product, the functionality-average functionality must be used). It is given by<sup>29</sup>

$$p_{\text{gel}} = 1/[(3.25 - 1)(2 - 1)]^{1/2} = 0.67$$

which is in very good agreement with the experimental value.

Taking into account that the time to gel at 125 °C (after the mixing period), was comprised between 20 and 25 min, the cure cycle described in the Experimental Section was selected (30 min at 115 °C followed by 60 min at 125 °C).

The synthesis of the PGE-modified epoxy network was performed by adding the stoichiometric amount of DGEBA (1.5 mol per mole of BSA), to the reaction product between PGE and BSA. The reaction was carried out using the same thermal cycle than for the POSS-modified epoxy network. While POSS-modified epoxy networks were opaque, the reference network containing PGE instead of POSS, was transparent.

**Characterization of POSS-Modified and PGE-Modified Epoxy Networks.** SEM micrographs of the POSS-modified epoxy are shown in Figure 9, parts a–d. The heterogeneous material showed the presence of smooth and rough macrodomains (Figure 9, parts a and b). As will be discussed later, rough areas are POSS-rich regions (Figure 9c) and smooth areas correspond to epoxy-rich regions (Figure 9d). This primary phase separation occurred when adding DGEBA to the POSS–BSA precursor, and was fixed by the polymerization reaction. The origin of this primary phase separation may be the incompatibility between the isobutyl groups

of the POSS molecule with the aromatic epoxy–amine species. A secondary phase separation is observed in the smooth regions. Possibly, during the primary phase separation process, the epoxy-rich phase was enriched in DGEBA, BSA, and a fraction of BSA–(POSS) (the species with only one cube attached to BSA). In the course of the formation of the epoxy–amine network, POSS was phase separated from the epoxy-rich phase (smooth domains), leading to POSS-rich particles with sizes in the range 0.5–1  $\mu\text{m}$ . This size of dispersed-phase particles is characteristic of a polymerization-induced phase separation process.<sup>29</sup>

To prove that smooth regions could be associated with the epoxy-rich phase, a material containing 19 wt % POSS was generated by adding extra DGEBA and BSA to the POSS–BSA precursor, keeping overall stoichiometry. This material also exhibited the presence of macrodomains but with a major fraction of smooth domains, consistently with the increase in the fraction of DGEBA and BSA in the initial formulation. Local thermal analysis proved that the glass transition temperature of the smooth regions was close to the one of the neat DGEBA–BSA network, recorded by DSC.

Local thermal analysis was performed to investigate if POSS-rich domains were amorphous or crystalline. Most of the scanned surface revealed to be amorphous, exhibiting a softening interval in a broad temperature range (see Figure 10a for the material modified with 51.8% POSS). However, the presence of crystals with an onset melting temperature of 133 °C, was evidenced at a few particular positions (Figure 10b). This means that POSS-rich domains were generated by a liquid–liquid phase separation and that crystallization eventually occurred at a few locations when cooling from the reaction temperature.

DSC thermograms of the POSS-modified epoxy network are shown in Figure 11. The material obtained after the standard cure cycle exhibited a glass transition temperature,  $T_g = 106.5$  °C, defined at the midpoint of the transition. This is in good agreement with the onset softening value observed by the modulated local thermal analysis (LTA) of the sample. With the latter technique, softening was observed in a broad temperature range, probably because of the deformation of the amorphous POSS clusters. Dynamic mechanical spectra did not supply any other relevant information. A broad  $\tan \delta$  peak with a maximum at 103 °C was recorded.

A small melting peak was observed in the 140–145 °C range (marked by an arrow in the lower curve of Figure 11). This is consistent with the presence of a very small fraction of crystals recorded by the microthermal analyzer. A postcure at 140 °C during 22 h led to an increase in the glass transition temperature to 121 °C and the disappearance of any evidence of crystallinity. This is possibly the result of the reaction of free functionalities that were trapped in the POSS-rich domains at the end of the standard cure cycle.

These results show that it is not possible to generate a nanoscale dispersion of large amounts of a monofunctional POSS in a thermosetting polymer if the cubes are not functionalized with an organic group compatible with the polymer network (in our case, a possibility could be to replace the isobutyl groups by phenyl groups). The lack of compatibility induces phase separation of POSS-rich and epoxy/amine-rich phases.

The reference network, where POSS was replaced by PGE, exhibited a  $T_g = 111$  °C (second thermal scan after

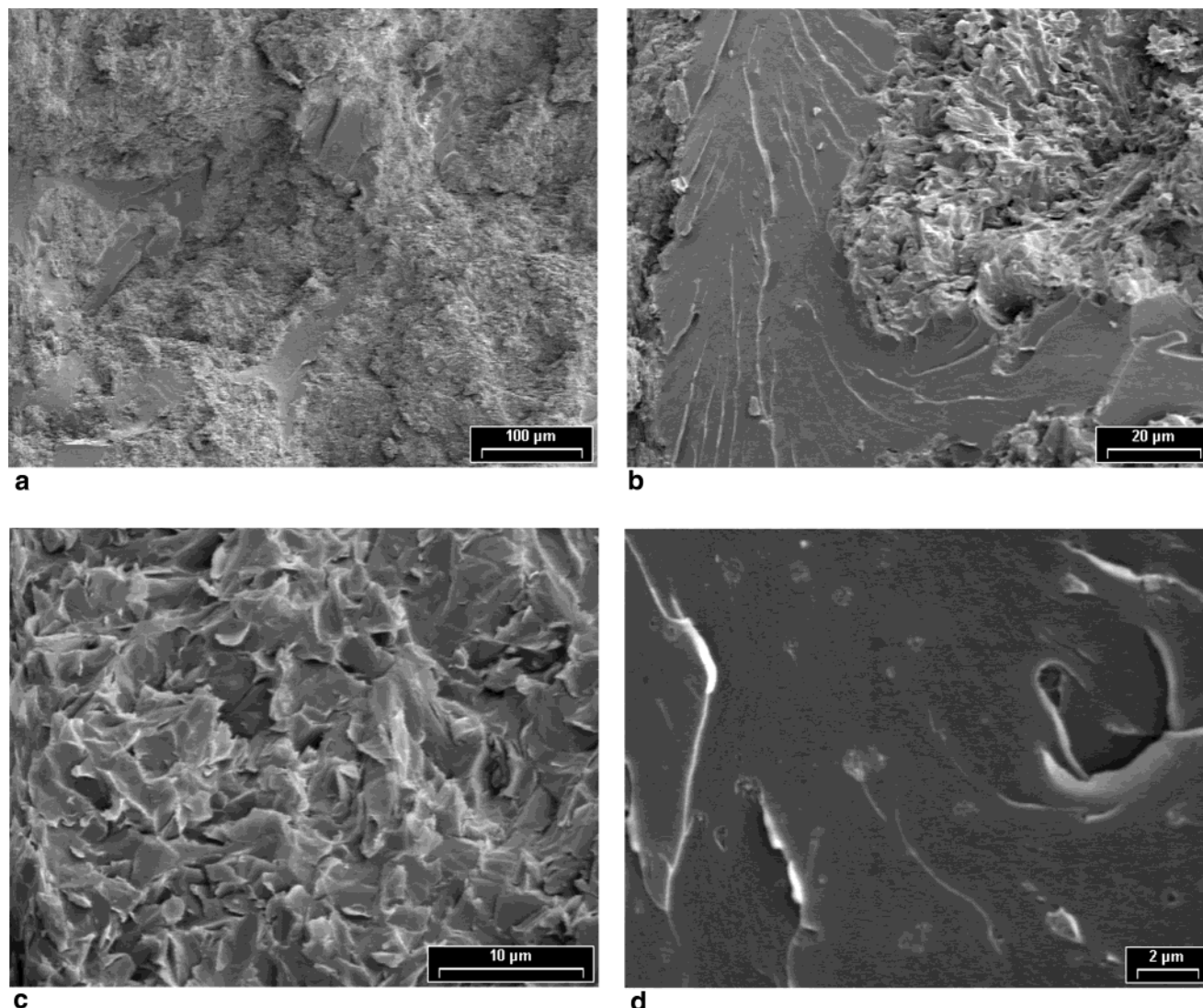


**Figure 9.** SEM micrographs of the POSS-modified epoxy network: (a) general view showing the presence of rough and smooth regions; (b) magnification of coexisting rough and smooth regions; (c) rough domains; (d) smooth domains showing a dispersion of small particles.

the standard cure cycle), 10 °C less than the POSS-modified epoxy after the postcure step. As both networks have the same topology, the higher  $T_g$  observed for the POSS-modified epoxy, may be associated with the hindering of polymer chain motions by their covalent bonding to POSS clusters.

For comparison purposes, the glass transition temperature of the stoichiometric DGEBA-BSA network was  $T_g = 140$  °C (second thermal scan after the standard cure cycle). This means that the decrease in  $T_g$  generated by the modification of network topology by partial replacement of DGEBA by a monofunctional epoxide, prevailed over the increase in  $T_g$  caused by the restriction of polymer chain motions produced by POSS clusters.

### Conclusions

Large mass fractions of a monofunctional POSS could be incorporated into an epoxy network following a two-step procedure. In a first step the POSS was completely reacted with a diamine, using a 1:1 molar ratio of both reactants. The resulting POSS-diamine precursor exhibited a distribution of species close to the ideal one. In a second step the POSS-diamine precursor was

reacted with a stoichiometric amount of a diepoxide leading to the final POSS-modified epoxy network. A primary liquid-liquid-phase separation process occurred at the time of adding the diepoxide to the POSS-diamine precursor, due to the lack of compatibility between the isobutyl groups present in the POSS molecule with the aromatic epoxy/amine species. This led to a macrophase separation into epoxy-rich and POSS-rich regions. A secondary phase separation occurred in the epoxy-rich phase in the course of polymerization, producing a dispersion of small POSS domains. Both LTA and DSC showed that most of POSS-rich domains were amorphous. No evidence of crystallinity was found after a postcure stage. A reference network was synthesized by replacing POSS by PGE in equimolar amounts. The resulting network was homogeneous but exhibited a lower glass transition temperature than the POSS-modified network. This is in agreement with results reported in the literature for epoxy networks modified with a small amount of a monofunctional POSS.<sup>26,27</sup>

The most important concept arising from these results is that a phase separation process may take place when employing a POSS bearing organic groups that are not



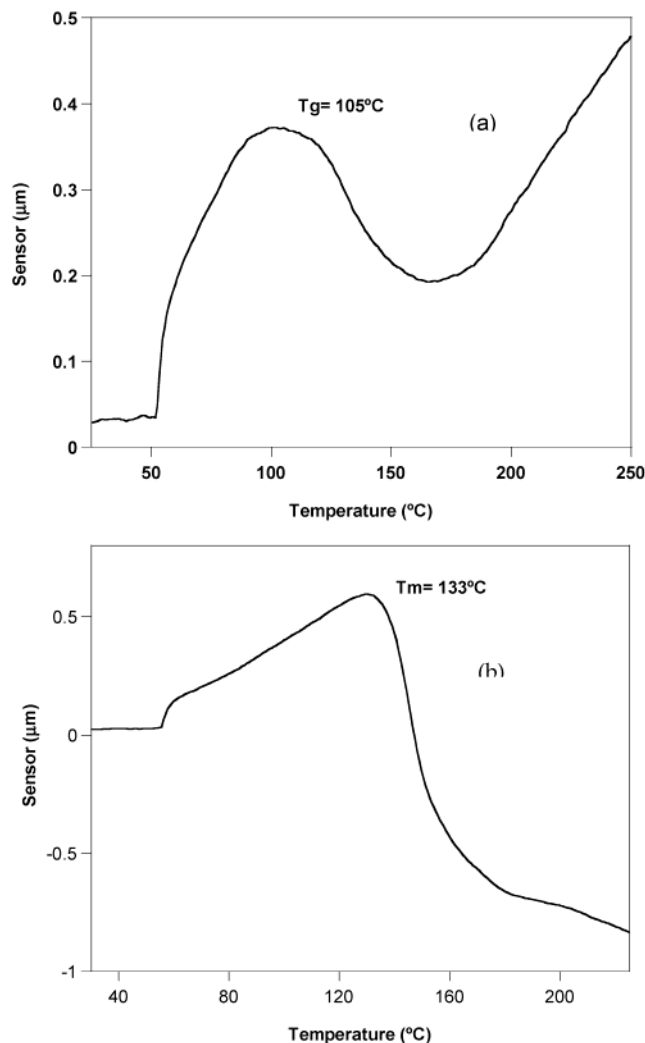


**Figure 10.** Local thermal analysis of the POSS-modified epoxy network (sensor signal vs temperature at a scan rate: 10 °C/s): (a) sensor signal observed in most of the sample surface; (b) sensor signal observed at a very few positions in the sample surface.

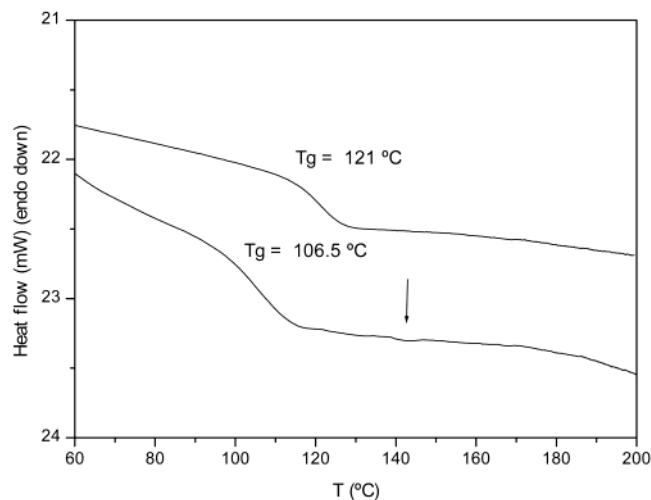


**Figure 11.** DSC thermograms of the POSS-modified epoxy network: lower curve, after the standard cure cycle; upper curve, after a postcure at 140 °C during 22 h.

compatible with the epoxy network. Our results also suggest that it should be possible to develop a formulation where the phase separation process takes place in

the course of polymerization, leading to a dispersion of POSS-rich microparticles in the thermosetting polymer (the morphology observed in the smooth domains). The in situ generation of a reinforced polymer might have practical applications.

**Acknowledgment.** The authors gratefully acknowledge financial support from CONICET and ANPCyT (Argentina), and from Comision Interministerial de Ciencia y Tecnología (CICYT) through Grant MAT 2000-0470 (Spain). Part of this work was carried out during a postdoctoral appointment of M.J.A. at INTEMA. The financial support of Secretaría Xeral de Investigación e Desenvolvemento (Xunta de Galicia), for this appointment, is gratefully acknowledged.

## References and Notes

- (1) Scott, D. W. *J. Am. Chem. Soc.* **1946**, *68*, 356.
- (2) Voronkov, M. G.; Lavrent'yev, V. I. *Top. Curr. Chem.* **1982**, *102*, 199.
- (3) Feher, F. J.; Weller, K. J. *Inorg. Chem.* **1991**, *30*, 689.
- (4) Lichtenhan, J. D.; Vu, N. Q.; Carter, J. A.; Gilman, J. W.; Feher, F. J. *Macromolecules* **1993**, *26*, 2141.
- (5) Sellinger, A.; Laine, R. M.; Chu, V.; Viney, C. *J. Polym. Sci., Part A: Polym. Chem.* **1994**, *32*, 3069.
- (6) Lichtenhan, J. D. *Comments Inorg. Chem.* **1995**, *17*, 115.
- (7) Haddad, T. S.; Lichtenhan, J. D. *J. Inorg. Organomet. Polym.* **1995**, *5*, 237.
- (8) Feher, F. J.; Weller, K. J.; Schwab, J. J. *Organometallics* **1995**, *14*, 2009.
- (9) Gilman, J. W.; Schlitzer, D. S.; Lichtenhan, J. D. *J. Appl. Polym. Sci.* **1996**, *60*, 591.
- (10) Lichtenhan, J. D.; Otonari, Y. A.; Carr, M. J. *Macromolecules* **1995**, *28*, 8435.
- (11) Haddad, T. S.; Lichtenhan, J. D. *Macromolecules* **1996**, *29*, 7302.
- (12) Tsuchida, A.; Bolln, C.; Sernetz, F. G.; Frey, H.; Mülhaupt, R. *Macromolecules* **1997**, *30*, 2818.
- (13) Romo-Urbe, A.; Mather, P. T.; Haddad, T. S.; Lichtenhan, J. D. *J. Polym. Sci., Part B: Polym. Phys.* **1998**, *36*, 1857.
- (14) Mather, P. T.; Jeon, H. G.; Romo-Urbe, A.; Haddad, T. S.; Lichtenhan, J. D. *Macromolecules* **1999**, *32*, 1194.
- (15) Bharadwaj, B. K.; Berry, R. J.; Farmer, B. L. *Polymer* **2000**, *41*, 7209.
- (16) Jeon, H. G.; Mather, P. T.; Haddad, T. S. *Polym. Int.* **2000**, *49*, 453.
- (17) Fu, B. X.; Hsiao, B. S.; White, H.; Rafailovich, M.; Mather, P. T.; Jeon, H. G.; Phillips, S.; Lichtenhan, J.; Schwab, J. *Polym. Int.* **2000**, *49*, 437.
- (18) Fu, B. X.; Hsiao, B. S.; Pagola, S.; Stephens, P.; White, H.; Rafailovich, M.; Sokolov, J.; Mather, P. T.; Jeon, H. G.; Phillips, S.; Lichtenhan, J.; Schwab, J. *Polymer* **2001**, *42*, 599.
- (19) Zheng, L.; Farris, R. J.; Coughlin, E. B. *J. Polym. Sci., Part A: Polym. Chem.* **2001**, *39*, 2920.
- (20) Zheng, L.; Farris, R. J.; Coughlin, E. B. *Macromolecules* **2001**, *34*, 8034.
- (21) Costa, R. O. R.; Vasconcelos, W. L.; Tamaki, R.; Laine, R. M. *Macromolecules* **2001**, *34*, 5398.
- (22) Sellinger, A.; Laine, R. M. *Macromolecules* **1996**, *29*, 2327.
- (23) Sellinger, A.; Laine, R. M. *Macromolecules* **1996**, *8*, 1592.
- (24) Zhang, C.; Babonneau, F.; Bonhomme, C.; Laine, R. M.; Soles, C. L.; Hristov, H. A.; Yee, A. F. *J. Am. Chem. Soc.* **1998**, *120*, 8380.
- (25) Li, G. Z.; Wang, L.; Toghiani, H.; Daulton, T. L.; Koyama, K.; Pittman, C. U., Jr. *Macromolecules* **2001**, *34*, 8686.
- (26) Lee, A.; Lichtenhan, J. D. *Macromolecules* **1998**, *31*, 4970.
- (27) Lee, A.; Lichtenhan, J. D. *J. Appl. Polym. Sci.* **1999**, *73*, 1993.
- (28) Barral, L.; Cano, J.; Díez, F. J.; Ramirez, C.; Abad, M. J.; Ares, A. *J. Polym. Sci., Part B: Polym. Phys.* **2002**, *40*, 284.
- (29) Pascault, J. P.; Sautereau, H.; Verdu, J.; Williams, R. J. J. *Thermosetting Polymers*; Dekker: New York, 2002.
- (30) Verchère, D.; Sautereau, H.; Pascault, J. P.; Riccardi, C. C.; Moschiar, S. M.; Williams, R. J. J. *Macromolecules* **1990**, *23*, 725.